Dynamic Extension Algorithm Based Tracking Control of STATCOM Via Port-Controlled Hamiltonian System

Gui, Yonghao; Chung, Chung Choo; Blaabjerg, Frede; Taul, Mads Graungaard

Published in:
I E E E Transactions on Industrial Informatics

DOI (link to publication from Publisher):
10.1109/TII.2019.2957038

Publication date:
2020

Document Version
Accepted author manuscript, peer reviewed version

Dynamic Extension Algorithm Based Tracking Control of STATCOM Via Port-Controlled Hamiltonian System

Yonghao Gui, *Member, IEEE*, Chung Choo Chung, *Member, IEEE*, Frede Blaabjerg, *Fellow, IEEE*, and Mads Graungaard Taul, *Student Member, IEEE*.

***Abstract*—A novel passivity-based control strategy is proposed for the exponentially stable tracking controller design of static synchronous compensator (STATCOM) system, which is a single input and single output. The STATCOM is not an input-affine system but a special port-controlled Hamiltonian system form. Hence, it is regularized by using a dynamic extension algorithm so that the proposed tracking control strategy is designed in an input-output linearization framework with a bounded solution to the driven zero dynamics equation. The proposed control strategy is proposed with consideration of the performance and stability of the input-output linearized dynamics. Simulation results show that the proposed control strategy improves the transient performance of the system compared to the previous results even in the lightly damped operating range.**

***Index Terms*—STATCOM. dynamic extension algorithm, input-output linearization, port-controlled Hamiltonian, exponentially stable.**

NOMENCLATURE

System Variables

$'$	Parameters and state variables with an apostrophe represent the per-unit values
α	Phase shift angle by which $e_{a,b,c}$ lead $V_{a,b,c}$
ω	Angular speed of the fundamental frequency voltage component
ω_b	Angular velocity at the system nominal frequency
C	Dc-link capacitor
$e_{a,b,c}$	Converter voltages
$i_{a,b,c}$	Three phase currents flowing through the lines
i_{dc}, V_{dc}	Dc-link current and voltage
I_d, I_q	Active (d-axis) and reactive (q-axis) currents
k	Factor relates the dc-link voltage to the maximum amplitude of $e_{a,b,c}$
L	Leakages of power transformers
R_p	Switching losses in the system
R_s	Conduction losses between the transformer and the inverter
$V_{a,b,c}$	Line voltages

Control Variables

a	Subscript 'a' indicates extended system's variable
d	Superscript 'd' indicates desired value
e	error
f, g, h	Smooth funcitons
H	Hamiltonian function
U, X, Y	Input, state, and output sets
$x, x(t)$	System state
y	System output

This research was supported by Korea Electric Power Corporation. (Grant number: R17XA05-56). (*Corresponding Author: Chung Choo Chung*.)

Y. Gui is with the Automation & Control Section at Department of Electronic Systems, Aalborg University, 9220 Aalborg, Denmark. He was on leave from the the Department of Electrical Engineering, Hanyang University, Seoul, Korea (e-mail: yg@es.aau.dk).

C. C. Chung is with the Division of Electrical and Biomedical Engineering, Hanyang University, Seoul 04763, Korea (e-mail: cchung@hanyang.ac.kr).

F. Blaabjerg and M. G. Taul are with the Department of Energy Technology, Aalborg University, 9220 Aalborg, Denmark (e-mail: fbl@et.aau.dk; mkg@et.aau.dk;).

I. INTRODUCTION

POWER converters are widely used in various applications such as flexible AC transmission systems (FACTS), renewable energy sources, and microgrids [1]–[5]. Static synchronous compensator (STATCOM), which is typically based on gate turnoff thyristors (GTO), are popular devices in FACTS and can improve the power quality and enhance the voltage stability by injecting or absorbing reactive power in the grid [6]–[8]. Compared to pulse-width modulation STATCOMs, it has a limited control input, phase angle, at which the STATCOM output voltage leads the bus voltage [8]–[10]. In this paper, a GTO-STATCOM using multi-pulse technology is studied due to its lower losses and lower harmonic contents [8]. For this type of STATCOM, there is little phase margin and/or lightly damped internal dynamics when using the input-output linearization (IOL) control strategy [8], [11]–[13].

To overcome these problems, various controllers have been proposed with the consideration of the system's characteristics. Schauder and Mehta designed a synthesized feedback control strategy using a proportional-plus-integral (PI) controller to obtain an improved phase margin in the inductive operating mode [11]. Petitclair *et al.* designed an IOL controller with an additional damping term for the STATCOM system, where the oscillation amplitude of the internal dynamics (dc-link voltage and active current) is effectively decreased [12]. Recently, Han *et al.* proposed an IOL with modified damping (IOLMD) controller to enhance the performance and stability of the active current and dc-link voltage dynamics with a nonlinear gain [14]. Due to the modified damping of the

IOLMD control strategy, we can move the eigenvalues of the internal dynamics further away from the imaginary axis [15]. Additionally, to guarantee that the damped internal dynamics is semi-global exponentially stable, the sufficient conditions were investigated through a parameter-dependent Lyapunov function [16]. In [17], a nonlinear control based on feedback linearization was proposed to provide better controllability and performance. Although these methods improve the performance, they are sensitive to uncertainties [18]. Furthermore, unexpected oscillatory performances appear in the dc-link voltage and active current when the STATCOM system operates in the inductive mode, where it includes lightly damped internal dynamics.

To overcome these issues, a passivity-based control (PBC) strategy was developed with the consideration of the dissipation of STATCOM system [19]–[23]. PBC has a robustness feature and has been used in various applications such as power converter, electro-mechanical systems, and mechanical systems, etc. [24]–[29]. In [22], the PBC with nonlinear damping is designed for the STATCOM to improve its performance compared with the IOLMD. However, the controller was designed based on an assumption that the input is to be a small value within its operating range. It will lose the stability in the whole operating range. To overcome such problem, a controller should be proposed to obtain an improved transient performance and robustness of the system based on a non-approximated model.

In this paper, we propose a novel tracking control strategy for a STATCOM based on port-controlled Hamiltonian (PCH) system without an approximation. The proposed tracking controller guarantees the exponential stability of the closed-loop system through the properties of the dissipation and the interconnection structure. The most critical problem of the STATCOM is that it does not have a flat output. If a system has a flat output, a tracking controller for the desired output trajectory can be obtained from the flat output and its derivatives. However, when a system does not have a flat output and is an irregular system, some auxiliary state variables are added into the system in order to regularize it. This is helpful for obtaining a relative degree under some assumptions. Furthermore, if a relative degree of a system is well defined, where the system is not input-affine, then the internal dynamics will include the control input; that is not helpful for guaranteeing stability when the control input does not go to zero at infinite time [18]. For this type of system, the system is first regularized via the dynamic extension algorithm (DEA) method to make sure that it is changed into an input-affine system. Then, for the dynamics extended system that has a relative degree, it is treated within the framework of dynamic feedback linearization. The tracking control law can be generated with a bounded solution to the driven zero dynamics equation [30]. Finally, we can expect the output of the system with the proposed control strategy will track the trajectory that has been generated.

Consequently, the main contribution of the paper is summarized as follows:

1) A new framework for a STATCOM, which is a single input single output PCH system with a special form, to design an exponentially stable tracking controller is introduced;
2) The stability of the internal dynamics of the STATCOM after using the dynamic extension algorithm (DEA) method is analyzed;
3) The proposed tracking controller guarantees that the origin of the system error dynamics is exponentially stable by using the properties of the interconnection structure and the dissipation.

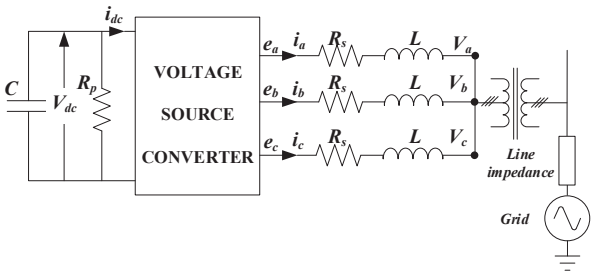

Fig. 1. Equivalent STATCOM circuit using a voltage source converter.

To validate the proposed method, we modified the demo model of Simcape Power Systems toolbox in MATLAB/Simulink, namely the "±100 Mvar 48-pulse GTO STATCOM". We modified the parameters and structure to accommodate ±100 Mvar 24-pulse STATCOM connected to a three-bus 345-kV, which was installed and has been in operation since 2009.

II. Model of STATCOM System

In this section, we introduce a STATCOM system to improve the power quality and enhance the voltage stability.

Fig. 1 shows an equivalent circuit of a STATCOM, which is connected to the transmission line through inductances in series. Consequently. a state-space model of the STATCOM system on the *d-q* frame could be represented as follows [11]:

$$\begin{aligned}\dot{x} &= f(x,\alpha)\\ &= \begin{bmatrix} -\frac{R_s'\omega_b}{L'}x_1 + \omega x_2 + \frac{k\omega_b}{L'}x_3\cos(\alpha) - \frac{\omega_b}{L'}|V'| \\ -\omega x_1 - \frac{R_s'\omega_b}{L'}x_2 + \frac{k\omega_b}{L'}x_3\sin(\alpha) \\ -\frac{3}{2}kC'\omega_b x_1\cos(\alpha) - \frac{3}{2}kC'\omega_b x_2\sin(\alpha) - \frac{\omega_b C'}{R_p'}x_3 \end{bmatrix},\\ y &= h(x) = x_2, \end{aligned} \tag{1}$$

where $x = \begin{bmatrix} x_1 & x_2 & x_3 \end{bmatrix}^T = \begin{bmatrix} I_d' & I_q' & V_{dc}' \end{bmatrix}^T$. $\alpha \in \mathbb{R}$ is the control input. Here $f : \mathbb{R}^3 \times \mathbb{R} \to \mathbb{R}^3$ is a sufficiently smooth function. An apostrophe in the parameters and state variables represents the per-unit value. The factor k is a constant in this system. When I_q' is a positive value, the STATCOM system operates in an inductive operation mode, i.e., it consumes the reactive power. When I_q' is a negative value, it operates in a capacitive operation mode, i.e., it supplies reactive power to the power network. In this study, the operating range of the STATCOM system is -1 pu $\le x_2 \le 1$ pu.

III. Controller Design Based on Port-Controlled System

In this section, firstly, the DEA method is used to regularize the system. Then, the proposed control strategy is designed with the consideration to the stability of the linearized dynamics. Moreover, the stability of the system is analyzed. Finally, we guarantee that the close-loop system is exponentially stable via the PCH method over the whole operating range.

A. Port-controlled Hamiltonian (PCH) systems [29]

Let $x \in \mathbb{R}^n$ and $u \in \mathbb{R}$ denote the state vector and the input, respectively. Consider a SISO system described in the state-space model as follows:

$$\begin{aligned} \dot{x} &= f(x,u) \\ y &= h(x), \end{aligned} \tag{2}$$

where $x \in X \subset \mathbb{R}^n$, $u \in U \subset \mathbb{R}$, and $y \in Y \subset \mathbb{R}$ are the state vector, the input, and the output, respectively. The functions $f(\cdot,\cdot) : X \times U \to \mathbb{R}^n$ and $h(\cdot) : X \to \mathbb{R}$ are sufficiently smooth in the open connected set X. Suppose that (2) satisfies the following PCH system such as

$$\dot{x} = (\mathfrak{R} + \mathfrak{J}(u)) \frac{\partial H(x)}{\partial x} + G(u), \tag{3}$$

where

$$\begin{aligned} &H(x) = \frac{1}{2} x^T S x, \quad S = S^T \succ 0, \\ &\mathfrak{R} = \mathfrak{R}^T \prec 0, \quad \mathfrak{J}^T(u) = -\mathfrak{J}(u). \end{aligned} \tag{4}$$

Here, the matrices S and $\mathfrak{R}$ are constant $n \times n$ matrices. $\mathfrak{R}$ is the dissipative forces in the system, $\mathfrak{J}(u)$ is the conservative forces, and $G(u)$ is the energy acquisition term [25].

Theorem 1: Suppose that there exist signals $u^d(t)$ and $x^d(t)$ that satisfy the PCH system in (3):

$$\dot{x}^d = \left(\mathfrak{R} + \mathfrak{J}(u^d)\right) \frac{\partial H(x^d)}{\partial x^d} + G(u^d). \tag{5}$$

If $u = u^d$ is applied to system in (3), then the tracking error dynamics becomes globally and exponentially stable. Namely, $\lim_{t\to\infty} \| x^d(t) - x(t) \| = 0$. ◊

Proof: Let $x(t) \in X \subset \mathbb{R}^n$ be the trajectory of (3) corresponding to an input, $u = u^d \in U \subset \mathbb{R}$, such that

$$\dot{x} = \left(\mathfrak{R} + \mathfrak{J}(u^d)\right) \frac{\partial H(x)}{\partial x} + G(u^d).$$

In general, $x^d(t)$ and $x(t)$ are different signals due to their different initial conditions, even though they satisfy the same PCH system in (3). If we define the error as $e := x^d - x$, we can obtain the tracking error dynamics as follows:

$$\dot{e} = \dot{x}^d - \dot{x} = \left(\mathfrak{R} + \mathfrak{J}(u^d)\right) \frac{\partial H(e)}{\partial e},$$

where H is defined in (4), If we use $H(e)$ as a Lyapunov function candidate, then derivative of $H(e)$ with respect to the time is given by

$$\begin{aligned} \dot{H}(e) &= \frac{1}{2} \left(\dot{e}^T \left(\frac{\partial H(e)}{\partial e} \right) + \left(\frac{\partial H(e)}{\partial e} \right)^T \dot{e} \right) \\ &= e^T S^T \mathfrak{R} S e. \end{aligned}$$

Here, $S = S^T \succ 0$ and $\mathfrak{R} \prec 0$, thus, the error globally exponentially converges to zero. Hence, $\lim_{t\to\infty} \| x^d(t) - x(t) \| = 0$. ■

Remark 1: It should be noted that the control strategy proposed in Theorem 1 is an open-loop controller that takes the advantage of the strict passivity of a PCH system. ◊

B. Desired control input for STATCOM system

If the STATCOM system in (1) is a flat system, we can find flatness references from the flat outputs. However, since the output of this type of STATCOM does not satisfy the flatness condition, it is necessary to find a desired control input in order to apply Theorem 1. In this study, a new state and a new input are defined as follows:

$$x_4 := \sin\alpha, \quad u := \dot{\alpha}. \tag{6}$$

Then, the STATCOM system in (1) could be represented such as

$$\begin{aligned} \dot{x}_a &= f_a(x_a) + g_a(x_a) u \\ y &= h_a(x_a), \end{aligned} \tag{7}$$

where $f_a(x)$ and $g_a(x)$ are smooth vector fields, and $h_a(x)$ is a smooth function defined on an open set $\Omega_x \in \mathbb{R}^4$, and

$$f_a(x_a) = \begin{bmatrix} -\frac{R_s^{'}\omega_b}{L^{'}} x_1 + \omega x_2 + \frac{k\omega_b}{L^{'}} x_3 \sqrt{1 - x_4^2} - \frac{\omega_b}{L^{'}} |V^{'}| \\ -\omega x_1 - \frac{R_s^{'}\omega_b}{L^{'}} x_2 + \frac{k\omega_b}{L^{'}} x_3 x_4 \\ -\frac{3}{2} k C^{'} \omega_b x_1 \sqrt{1 - x_4^2} - \frac{3}{2} k C^{'} \omega_b x_2 x_4 - \frac{\omega_b C^{'}}{R_p^{'}} x_3 \\ 0 \end{bmatrix},$$

$$g_a(x_a) = \begin{bmatrix} 0 & 0 & 0 & \sqrt{1 - x_4^2} \end{bmatrix}^T, \; h_a(x_a) = x_2,$$

$$x_a = \begin{bmatrix} x_1 & x_2 & x_3 & x_4 \end{bmatrix}^T = \begin{bmatrix} I_d^{'} & I_q^{'} & V_{dc}^{'} & \sin\alpha \end{bmatrix}^T.$$

For the system in (7), we have

$$\begin{aligned} \frac{\partial h_a}{\partial x_a} &= (0 \; 1 \; 0 \; 0), \\ L_g h_a(x_a) &= 0, \\ L_f h_a(x_a) &= -\omega x_1 - \frac{R_s^{'}\omega_b}{L^{'}} x_2 + \frac{k\omega_b}{L^{'}} x_3 x_4, \\ \frac{\partial (L_f h_a)}{\partial x_a} &= \left(-\omega \; -\frac{R_s^{'}\omega_b}{L^{'}} \; \frac{k\omega_b}{L^{'}} x_4 \; \frac{k\omega_b}{L^{'}} x_3 \right), \\ L_g L_f h_a(x_a) &= \frac{k\omega_b}{L^{'}} x_3 \sqrt{1 - x_4^2}. \end{aligned} \tag{8}$$

Hence, the relative degree of the STATCOM system is two in $\mathbb{R}^4$. In order to establish a normal form, we set

$$\begin{aligned} z_1 &:= \phi_1(x_a) = h_a(x_a) = x_2, \\ z_2 &:= \phi_2(x_a) = L_f h_a(x_a) = -\omega x_1 - \frac{R_s^{'}\omega_b}{L^{'}} x_2 + \frac{k\omega_b}{L^{'}} x_3 x_4. \end{aligned} \tag{9}$$

We look for two functions ϕ_3 and ϕ_4 such that

$$\begin{aligned}\frac{\partial \phi_3}{\partial x_a} g_a(x_a) = \frac{\partial \phi_3}{\partial x_4}\sqrt{1-x_4^2} = 0,\\ \frac{\partial \phi_4}{\partial x_a} g_a(x_a) = \frac{\partial \phi_4}{\partial x_4}\sqrt{1-x_4^2} = 0.\end{aligned} \tag{10}$$

Two new variables could be defined as follows:

$$z_3 := \phi_3(x_a) = x_1, \quad z_4 := \phi_4(x_a) = x_3. \tag{11}$$

A transformation can be defined by using (11) and the previous two functions in (9) as $z = \begin{bmatrix} z_1 & z_2 & z_3 & z_4 \end{bmatrix}^T = \Phi(x_a)$. Its Jacobian matrix is

$$\frac{\partial \Phi}{\partial x_a} = \begin{bmatrix} 0 & 1 & 0 & 0 \\ -\omega & -\frac{R_s^{'}\omega_b}{L^{'}} & \frac{k\omega_b}{L^{'}}x_4 & \frac{k\omega_b}{L^{'}}x_3 \\ 1 & 0 & 0 & 0 \\ 0 & 0 & 1 & 0 \end{bmatrix}. \tag{12}$$

Remark 2: Notice that, (12) is nonsingular in the whole operating range since $x_3 = z_4 \neq 0$. $\Diamond$

Consequently, $\Phi(x_a)$ is a local diffeomorphism [18]. The inverse transformation could be obtained such as

$$x_1 = z_4. \quad x_2 = z_1, \quad x_3 = z_3, \quad x_4 = \frac{z_2 + \omega z_3 + \frac{R_s^{'}\omega_b}{L^{'}} z_1}{\frac{k\omega_b}{L^{'}} z_4}. \tag{13}$$

The STATCOM system can be described in the new coordinates by

$$\begin{aligned}\dot{z}_1 &= z_2\\ \dot{z}_2 &= b(z) + a(z)u\\ \dot{z}_3 &= -\frac{R_s^{'}\omega_b}{L^{'}} z_3 + \omega z_1 + \frac{k\omega_b}{L^{'}} z_4 q_c(z) - \frac{\omega_b}{L^{'}}|V^{'}|\\ \dot{z}_4 &= -\frac{3}{2}kC^{'}\omega_b z_3 q_c(z) - \frac{3}{2}kC^{'}\omega_b z_1 q_s(z) - \frac{\omega_b C^{'}}{R_p^{'}} z_4,\end{aligned} \tag{14}$$

where

$$\begin{aligned}b(z) &= -\omega\left(-\frac{R_s^{'}\omega_b}{L^{'}} z_3 + \omega z_1 + \frac{k\omega_b}{L^{'}} z_4 q_c(z) - \frac{\omega_b}{L^{'}}|V^{'}|\right)\\ &\quad - \frac{R_s^{'}\omega_b}{L^{'}}(z_2) + \frac{k\omega_b}{L^{'}} q_s(z)\left(-\frac{3}{2}kC^{'}\omega_b z_3 q_c(z)\right.\\ &\quad \left. - \frac{3}{2}kC^{'}\omega_b z_1 q_s(z) - \frac{\omega_b C^{'}}{R_p^{'}} z_4\right),\\ a(z) &= \frac{k\omega_b}{L^{'}} z_4 q_c(z), \quad q_c(z) = \sqrt{1-q_s(z)^2},\\ q_s(z) &= \frac{z_2 + \omega z_3 + \frac{k\omega_b}{L^{'}} z_1}{\frac{k\omega_b}{L^{'}} z_4}.\end{aligned}$$

If we give the desired output, z_1^d, then we can calculate the other desired states based on the system dynamics in (14) in the new coordinates such as

$$\begin{aligned}z_2^d &= \dot{z}_1^d\\ \dot{z}_3^d &= -\frac{R_s^{'}\omega_b}{L^{'}} z_3^d + \omega z_1^d + \frac{k\omega_b}{L^{'}} z_4^d q_c(z^d) - \frac{\omega_b}{L^{'}}|V^{'}|\\ \dot{z}_4^d &= -\frac{3}{2}kC^{'}\omega_b z_3^d q_c(z^d) - \frac{3}{2}kC^{'}\omega_b z_1^d q_s(z^d) - \frac{\omega_b C^{'}}{R_p^{'}} z_4^d,\end{aligned} \tag{15}$$

where

$$q_c(z^d) = \sqrt{1-q_s(z^d)^2}, \quad q_s(z^d) = \frac{z_2^d + \omega z_3^d + \frac{k\omega_b}{L^{'}} z_1^d}{\frac{k\omega_b}{L^{'}} z_4^d}.$$

Thus, the desired input can be obtained based on (14) and (15) as follows:

$$u^d = \frac{-b(z^d) + \nu}{a(z^d)}, \tag{16}$$

where

$$\nu = \ddot{z}_1^d - K_1(\dot{z}_1 - \dot{z}_1^d) - K_2(z_1 - z_1^d). \tag{17}$$

Remark 3: z_1^d is generated by the 5$^{\text{th}}$ profile, $K_1 > 0$ and $K_2 > 0$. Notice that $a(z^d) \neq 0$ for all operating points; this is the case because $z_4^d = x_3^d \neq 0$ and $q_c(z^d) = \cos^2(\alpha^d) \neq 0$. $\Diamond$

C. Stability analysis of internal dynamics

In practical systems, the global Lipschitz hypothesis for the zero dynamics is a strong assumption [30]. Although Lipschitz condition of zero dynamics for the STATCOM system is shown in [15], the bound of the states of internal dynamics is directly presented by using Lyapunov theorem in this subsection. To simplify analysis, the equilibrium points are moved to the origin:

$$\tilde{z}_i := z_i^d - z_{i,o}, \tag{18}$$

where $i = 3, 4$, and $z_{i,o}$ are operating points. We take a Lyapunov function candidate, as follows:

$$V_{int} = \frac{1}{2}\tilde{z}_3^2 + \frac{1}{3L^{'}C^{'}}\tilde{z}_4^2. \tag{19}$$

The time derivative of (19) can be obtained.

$$\begin{aligned}\dot{V}_{int} &= -\frac{2\omega_b}{3LR_p^{'}}\tilde{z}_4^2 - \frac{2\omega_b}{3LR_p^{'}} z_{4,o}\tilde{z}_4 - \frac{R_s^{'}\omega_b}{L^{'}}\tilde{z}_3^2 - \frac{R_s^{'}\omega_b}{L^{'}} z_{3,o}\tilde{z}_3\\ &\quad - \frac{k\omega_b}{L^{'}} q_c(z^d)(z_{3,o}\tilde{z}_4 - z_{4,o}\tilde{z}_3)\\ &\quad - \frac{k\omega_b}{L^{'}} z_{1,o} q_s(z^d)\tilde{z}_4 + \omega z_{1,o}\tilde{z}_3 - \frac{\omega_b}{L^{'}}|V^{'}|\tilde{z}_3.\end{aligned} \tag{20}$$

Assumption 1: For simplicity of analysis, we assume that there exists θ such that $0 \leq \theta_c \leq \theta < 1$ and $-\theta \leq \theta_s \leq \theta$ in the operating range.

$$q_c(z^d) = 1 - \theta_c. \quad q_s(z^d) = \theta_s. \tag{21}$$

$\Diamond$

Assumption 1 is acceptable in this paper, because the magnitude of α is sufficiently small in the operating range. In addition, $q_c(z^d)$ is the cosine of α^d and $q_s(z^d)$ is the sine of α^d. Thus, (20) can be rewritten as follows:

$$\begin{aligned}\dot{V}_{int} &= -\frac{2\omega_b}{3LR_p^{'}}\tilde{z}_4^2 - \left(\frac{2\omega_b}{3LR_p^{'}} z_{4,o} + \frac{k\omega_b}{L^{'}} z_{1,o}\theta_s + \frac{k\omega_b}{L^{'}} z_{3,o}\right)\tilde{z}_4\\ &\quad - \frac{R_s^{'}\omega_b}{L^{'}}\tilde{z}_3^2 - \left(\frac{R_s^{'}\omega_b}{L^{'}} z_{3,o} - \omega z_{1,o} + \frac{k\omega_b}{L^{'}} z_{4,o} + \frac{\omega_b}{L^{'}}|V^{'}|\right)\tilde{z}_3\\ &\quad + \frac{k\omega_b}{L^{'}}\theta_c(z_{3,o}\tilde{z}_4 - z_{4,o}\tilde{z}_3).\end{aligned} \tag{22}$$

We assume $q_c(z_o) = 1 - \theta_{c.o}$ and $q_s(z_o) = \theta_{s.o}$, which allows us to obtain two equality equations from (15) as follows:

$$\begin{aligned} 0 &= -\frac{3}{2}kC^{'}\omega_b z_{3,o}(1-\theta_{c.o}) - \frac{3}{2}kC^{'}\omega_b z_{1,o}\theta_{s.o} - \frac{\omega_b C^{'}}{R_p^{'}} z_{4,o} \\ 0 &= -\frac{R_s^{'}\omega_b}{L^{'}} z_{3,o} + \frac{k\omega_b}{L^{'}} z_{4,o}(1-\theta_{c.o}) - \frac{\omega_b}{L^{'}}|V^{'}|, \end{aligned} \tag{23}$$

Consequently, (22) can be represented such as

$$\begin{aligned} \dot{V}_{int} = &-\frac{2\omega_b}{3LR_p^{'}}(\tilde{z}_4 - \frac{3kR_p^{'}}{4}(\tilde{\theta}_s z_{1,o} + \tilde{\theta}_c z_{3,o}))^2 \\ &- \frac{R_s^{'}\omega_b}{L^{'}}(\tilde{z}_3 + \frac{k}{2R_s^{'}}\tilde{\theta}_c z_{4,o})^2 \\ &+ \frac{3k^2 R_p^{'}\omega_b}{8L^{'}}(\tilde{\theta}_s z_{1,o} + \tilde{\theta}_c z_{3,o})^2 + \frac{k^2\omega_b}{4R_s^{'}L^{'}}\tilde{\theta}_c^2 z_{4,o}^2. \end{aligned} \tag{24}$$

Thus, $\dot{V}_{int}$ is negative in the set $\{\tilde{z} : |\tilde{z}_3| \geq (1+\varepsilon)\frac{k}{R_s^{'}}(-\tilde{\theta}_c)z_{4,o}\} \cap |\tilde{z}_4| \geq (1+\varepsilon)\frac{3kR_p^{'}}{2}(\tilde{\theta}_s z_{1,o} + \tilde{\theta}_c z_{3,o})$, where $\tilde{\theta}_s = \theta_s - \theta_{s,o}$, $\tilde{\theta}_c = \theta_c - \theta_{c,o}$, and $\varepsilon > 0$.

D. Port-controlled Hamiltonian form for STATCOM

If we take a Hamiltonian function for the STATCOM system in (1) such that

$$H(x) = \frac{1}{2}x^T S x \tag{25}$$

where

$$S = \begin{bmatrix} 1 & 0 & 0 \\ 0 & 1 & 0 \\ 0 & 0 & \frac{2}{3L^{'}C^{'}} \end{bmatrix},$$

then the STATCOM system in (1) is changed into form in (3),

$$\dot{x} = (\mathfrak{R} + \mathfrak{J}(\alpha))\frac{\partial H(x)}{\partial x} + G, \tag{26}$$

where

$$\mathfrak{R} = \begin{bmatrix} -\frac{R_s^{'}\omega_b}{L^{'}} & 0 & 0 \\ 0 & -\frac{R_s^{'}\omega_b}{L^{'}} & 0 \\ 0 & 0 & -\frac{3\omega_b L^{'}C^{'2}}{2R_p^{'}} \end{bmatrix}, \quad G = \begin{bmatrix} -\frac{\omega_b}{L^{'}}|V^{'}| \\ 0 \\ 0 \end{bmatrix},$$

$$\mathfrak{J}(\alpha) = \begin{bmatrix} 0 & \omega & \frac{3}{2}kC^{'}\omega_b\cos(\alpha) \\ -\omega & 0 & \frac{3}{2}kC^{'}\omega_b\sin(\alpha) \\ -\frac{3}{2}kC^{'}\omega_b\cos(\alpha) & -\frac{3}{2}kC^{'}\omega_b\sin(\alpha) & 0 \end{bmatrix}.$$

Thus, we design a desired input based on (6) and (16):

$$\alpha^d = \int_0^t u^d(t)dt, \tag{27}$$

which satisfies the dynamics in (5). If $\alpha = \alpha^d$ is taken for the STATCOM system, then the closed-loop system is exponentially stable based on Theorem 1. The whole procedure of the proposed control strategy is illustrated in Fig. 2.

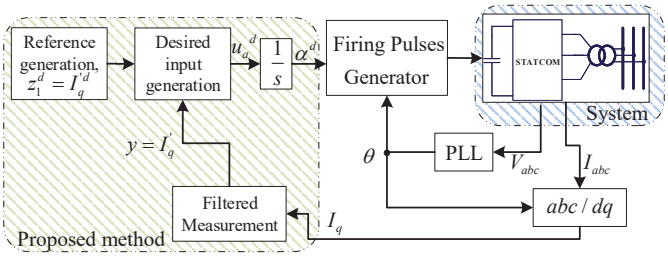

Fig. 2. Controller block diagrams of the proposed method.

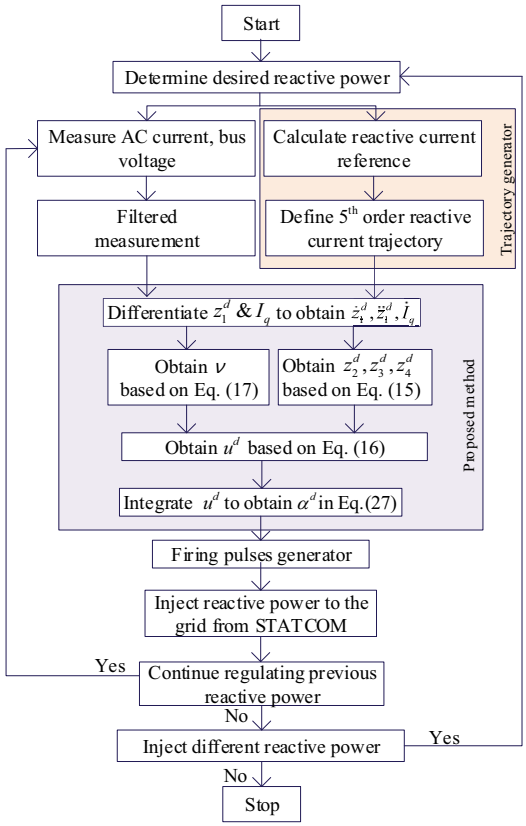

Fig. 3. Flowchart of the proposed control strategy.

E. Flowchart of the proposed control strategy

An exemplary flowchart of the proposed control strategy is shown in Fig. 3. The proposed control strategy process begins at start. Regarding the desired reactive power, $Q_{ref}^{'}$, the reference of $I_q^{'}$, $I_{qref}^{'}$, is calculated via 5^{th}-order trajectory. The line currents and bus voltages are meausred and filtered according to a desired sampling time. Then, $\dot{z}_1^d$, $\ddot{z}_1^d$, $\dot{I}_q^{'}$ are obtained by differencing z_1^d and $I_q^{'}$. The new feedback term, ν, is calculated by using (30), and the other states are calculated by using (15). The actual control input, α is calculated via (27). The STATCOM generates the reactive power to the grid through the firing pulses generator. Finally, if the STATCOM system generates the same $Q_{ref}^{'}$, then it regulates the previous reference. If the STATCOM continues to inject a different amount of $Q^{'}$, then the process returns to the determination of $Q_{ref}^{'}$. Otherwise, the STATCOM control is deactivated.

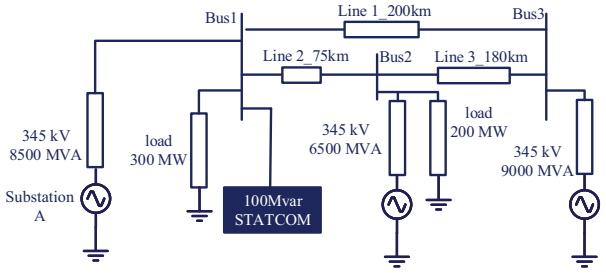

Fig. 4. Studied system with ±100 Mvar 24 pulse STATCOM.

IV. Performance Evaluation

We executed simulations to validate the effectiveness of the proposed control strategy in terms of the parameter uncertainties by using a switching model of the converter with simple switch models in Matlab/Simulink and Simscape Power Systems. Fig. 4 shows the test system, which is constructed based on a ±100 Mvar 24 pulse STATCOM generating/absorbing reactive power in a 345-kV system. The system parameters tested in the simulation are listed Table I, and the parameters of the transmission line could be referred in [22]. The control specifications of $I_q^{'}$ are as follows: the settling time is less than 16 *ms*, the overshoot is less than 0.1 *pu*, and the steady-state error is less than 0.05 *pu*. In this study, the operating range of $I_{q,ref}^{'}$ is from -1 *pu* to 1 *pu*. The proposed control algorithm is compared to the PI and IOLMD methods, where the PI method is designed as follows [11]:

$$\alpha = K_{P_{PI}}(x_2^* - x_2) + K_{I_{PI}} \int_0^t (x_2^* - x_2), \tag{28}$$

where x_2^* is the reference of x_2, and $K_{P_{PI}}$ and $K_{I_{PI}}$ are the PI controller gains. In addition, the IOLMD method is designed as follows [14]:

$$\alpha = \sin^{-1}\left[\frac{L'\left\{v_{IOL} + \omega x_1 + \frac{R_s'\omega_b x_2}{L'} + K_d\left(x_2 - \frac{2}{3kC'}x_3\right)(\dot{x}_1)\right\}}{k\omega_b x_3}\right], \tag{29}$$

where

$$v_{IOL} = K_{P_{IOL}}(x_2^* - x_2) + K_{I_{IOL}} \int_0^t (x_2^* - x_2),$$

where $K_{P_{IOL}}$ and $K_{I_{IOL}}$ are the PI controller gains, and K_{IOL} is the damping gain. In addition, it should be noted that, in order to remove the offset when there exist model uncertainties, an additional integrator term is added into the proposed method in (30) such as

$$v = \ddot{z}_1^d - K_1(\dot{z}_1 - \dot{z}_1^d) - K_2(z_1 - z_1^d) - K_3 \int_0^t (z_1 - z_1^d). \tag{30}$$

A. Tracking performance

Figs. 5(a), (b), and (c) show the transient response of the system in capacitive mode when $I_{q,ref}^{'}$ is changed from 0.8 pu to -0.8 pu. We observe that the performance with all three methods are similar in this operating range, where the STATCOM system has large damping analyzed in [22]. When $I_{q,ref}^{'}$ is changed from -0.8 pu to 0.8 pu, we observe that the performance of $I_q^{'}$ with all three methods are similar, as shown in Fig. 5(e). However, Figs. 5(d) and (f) show that the proposed control strategy indicated by the red dash-dotted line (PCH) has a smaller overshoot and faster convergence that other two methods because the proposed control strategy considers the system's inherent passivity property at this lightly damped operating point.

TABLE I
STATCOM System Parameters.

Parameter	Value	Unit	pu
AC voltage	345	kV_{LL}	1
Rating	100	Mvar	1
R_s	4.8	Ω	0.0071
R_p	1.7	kΩ	727.5846
C	0.4	mF	2.78
L	269.5	mH	0.15
k	0.6312		
ω	$2*\pi*60$	rad/sec	

TABLE II
Controller Gains Used in the Simulation.

Method	Values
PI	$K_{P_{PI}} = 10,\ K_{I_{PI}} = 20$
IOLMD	$K_{P_{IOL}} = 4000,\ K_{I_{IOL}} = 100,\ K_d = -0.03$
PCH	$K_1 = 500,\ K_2 = 8000,\ K_3 = 100$

B. Robustness performance

In this case, the magnitude of the network voltage $V^{'}$ was assumed to vary within the range of 95%–105% with regards to the power system conditions of the Korea Electric Power Corporation standard [14], [22]. $V^{'}$ was 1 pu from 0.5 s to 0.8 s, and decreased to 0.95 pu at 0.8 s, where maintained 0.95 pu within 0.3 s. Then, it stepped up to 1.05 pu at 1.1 s,

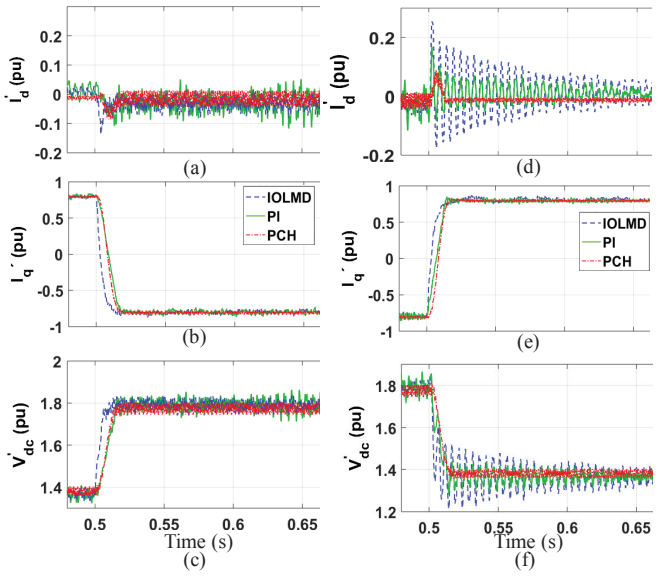

Fig. 5. Transient responses of the STATCOM system (a) $I_d^{'}$, (b) $I_q^{'}$, (c) $V_{dc}^{'}$ when $I_{q,ref}^{'}$ is changed from 0.8 pu to -0.8 pu, and (d) $I_d^{'}$, (e) $I_q^{'}$, (f) $V_{dc}^{'}$ when $I_{q,ref}^{'}$ is changed from -0.8 pu to 0.8 pu.

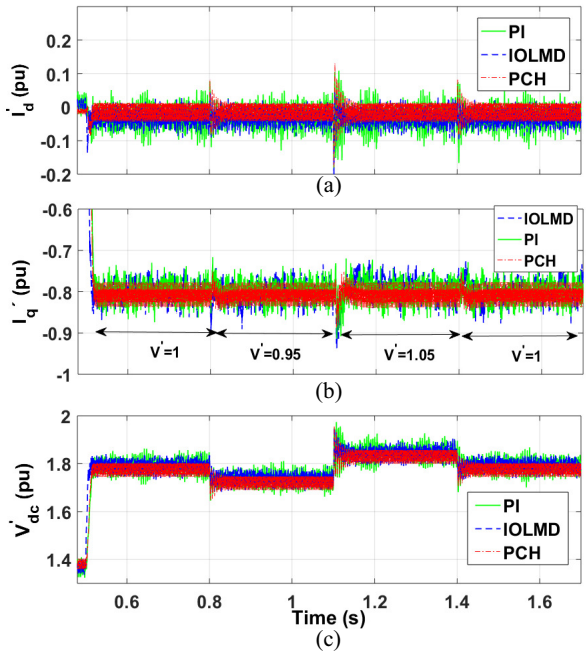

Fig. 6. Capacitive mode: Time responses of the STATCOM system when the network voltage $V^{'}$ varies in the range of 95–105%. (a) $I_d^{'}$, (b) $I_q^{'}$, (c) $V_{dc}^{'}$.

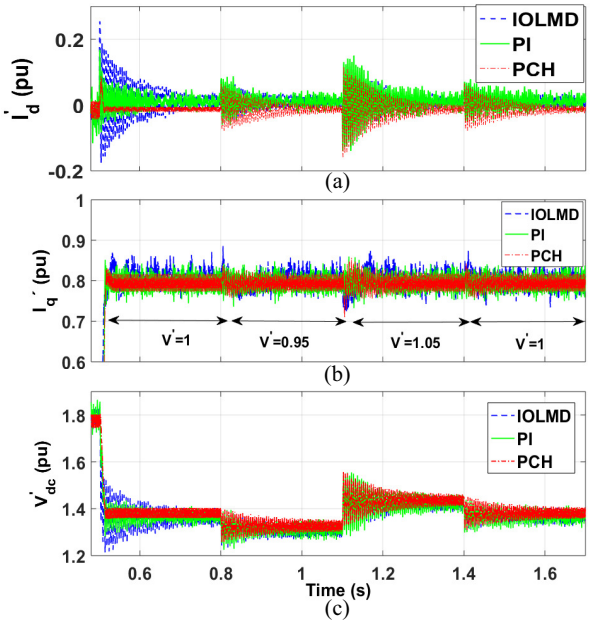

Fig. 7. Inductive mode: Time responses of the STATCOM when the network voltage $V^{'}$ varies in the range of 95–105%. (a) $I_d^{'}$, (b) $I_q^{'}$, (c) $V_{dc}^{'}$.

and went back to 1 pu at 1.4 s, at substation A under a modified transmission network.

Fig. 6 shows the performance of the STATCOM when it is working in the capacitive mode. All three methods have the similar performance because the system has enough damping. Fig. 7 shows the performance of the STATCOM when it is working in the inductive mode. In addition, Figs. 8 shows the voltage when the system is working in the capacitive and inductive modes. At the lightly damped operating point, the time

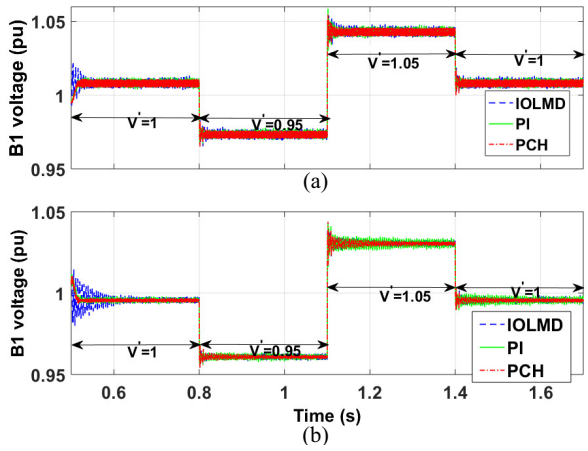

Fig. 8. Voltage at bus 1 (B1) when $V^{'}$ varies in the range of 95–105%. (a) Capacitive mode; (b) Inductive mode.

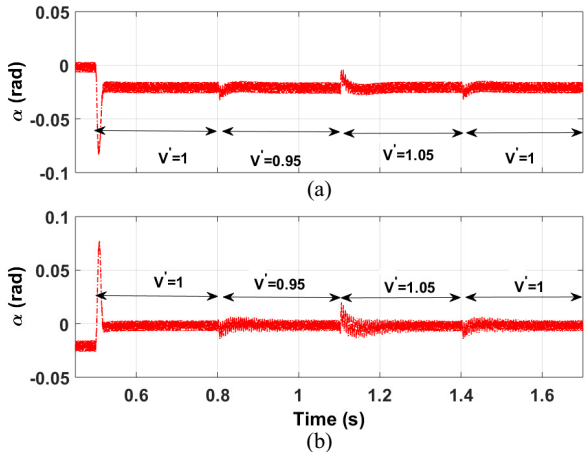

Fig. 9. Results of α when $V^{'}$ varies in the range of 95–105%. (a) Capacitive mode; (b) Inductive mode.

response of the proposed control strategy is slightly improved compared to that of the IOLMD and PI methods regarding to the network voltage variations since the objective of the proposed control strategy is designed without considering the improvement of the performance when the network voltage varies, but instead aims to regulate $I_q^{'}$. In addition, Fig. 9 shows the corresponding α of the proposed control strategy. We can expect that the performance could be improved with an additional nonlinear damping studied in the future.

We also tested the proposed control strategy in the presence of the variation of capacitance of the dc-link capacitor, which will change after a certain time. It is assumed that the capacitance is decreased to 70% of normal value. In this case, we tested the proposed control strategy only in the inductive operating mode, where the system has lightly damped dynamics. From Fig. 10(b), the tracking performance of I_q with the proposed control strategy is slightly depressed. However, dc voltage and active current converge their operating points faster than the IOLMD. In addition, we also tested the proposed control strategy in the inductive operating mode when there is $\pm 30\%$ of R_p parameter variation in the control implementation, as shown in Fig. 11. It can be observed that

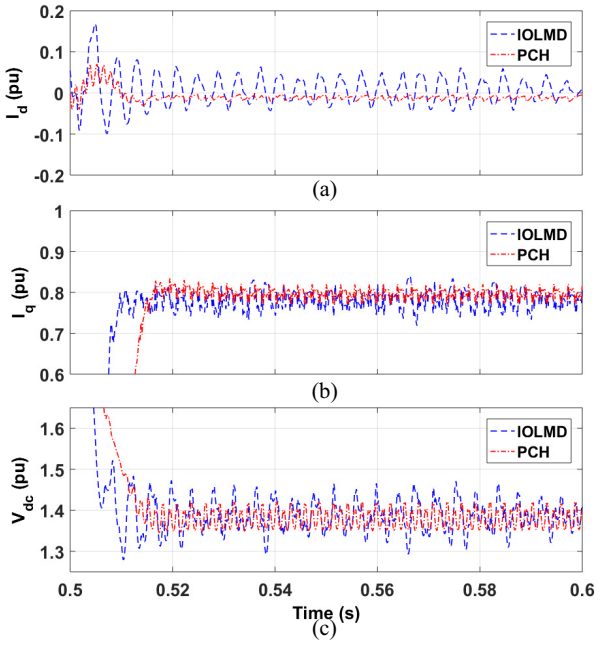

Fig. 10. Inductive mode: Transient responses of the STATCOM when the capacitance is decreased to 70% of normal. (a) $I_d^{'}$, (b) $I_q^{'}$, (c) $V_{dc}^{'}$.

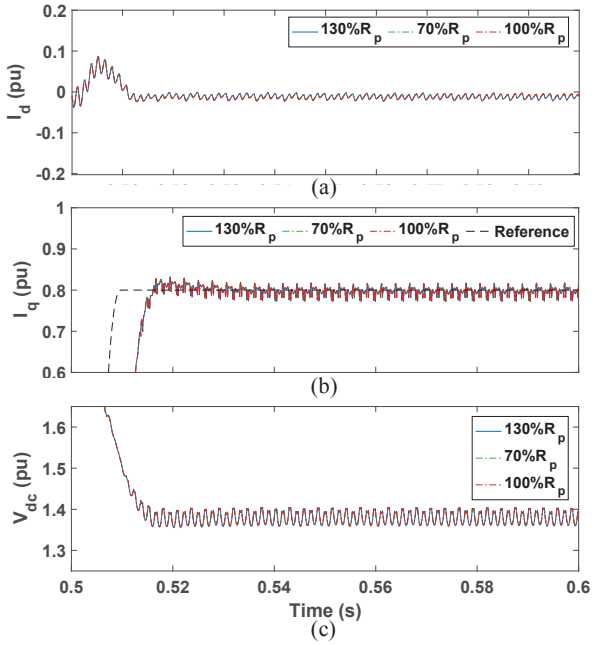

Fig. 11. Inductive mode:Transient responses of the STATCOM when R_p has $\pm$30% error in control implementation. (a) $I_d^{'}$, (b) $I_q^{'}$, (c) $V_{dc}^{'}$.

the performance with the proposed method is not affected by that parameter uncertainty. Consequently, we can conclude that the proposed method is robust to the parameter uncertainties.

Finally, we test a severe disturbance which occurs at substation A. At 0.5 s, the grid voltage decreases from 1.0 pu to 0.7 pu, and the disturbance is cleared after 2 cycles. Fig. 12 shows that the voltage cannot get back to 1.0 pu due to the limit of STATCOM capacity. The proposed control strategy is working well even the severe voltage occurs drops to 0.7 pu,

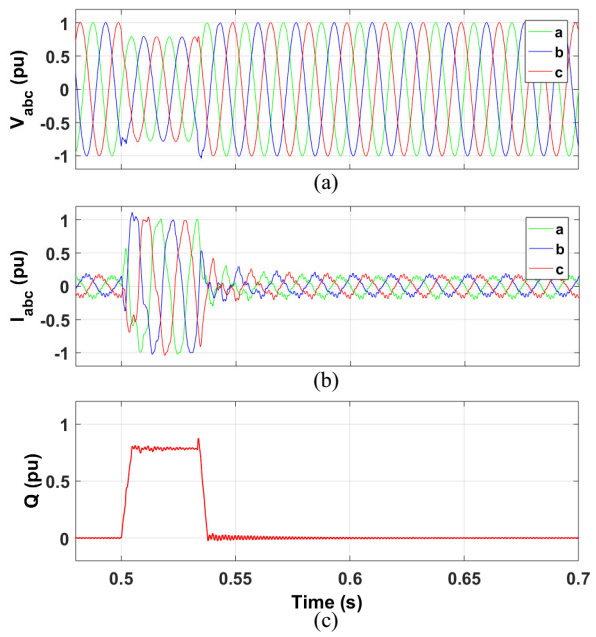

Fig. 12. Performance of the system, (a) voltages, (b) currents, and (c) output reactive power in a severe disturbance.

and goes back to its nominal value when the disturbance is cleared.

C. Experimental validation

The effectiveness of the proposed method was also validated by using a prototype experimental setup as a three-phase 7.5 kW voltage source converter (VSC) system, as shown in Fig. 13. We used a 6 mH L–filter to emulate the leakages of power transformers $L^{'}$. A grid simulator was used to support 200 V RMS grid voltage. The control strategies were implemented in the DS1007 dSPACE system, where the reference signal was modified in the ControlDesk. The grid voltages and the line currents were measured and sent to the controller by using a DS2004 A/D board. Finally, the switching pulses of the VSC were generated by using the DS5101 digital waveform output board. For over-voltage protection, a dc-chopper with a controllable brake resistor was included on the dc-link. It should be noted that all three methods are implemented in the PWM VSC, where k was set to a constant in order to emulate a multi-pulse STATCOM, since the phase shift transformer was not applicable in the lab. It is an acceptable way to validate the control strategy since the transformer is not an important part of the solution, but the control part is the important contribution in this paper.

Fig. 14 shows the measured performance when $I_{q,ref}^{'}$ is changed from -0.8 pu to 0.8 pu, it can be observed that the performances of three methods has the similar tendency compared with the simulation results in the capacitive mode (e.g., Figs. 5(a), (b), and (c)), since the damping of the system is increased due to the larger resistor of L filter and larger capacitance of dc-link capacitor, which are helpful to damp the oscillations in I_d and V_{dc} even in the inductive mode. In addition, Fig. 15 shows the measured performance when

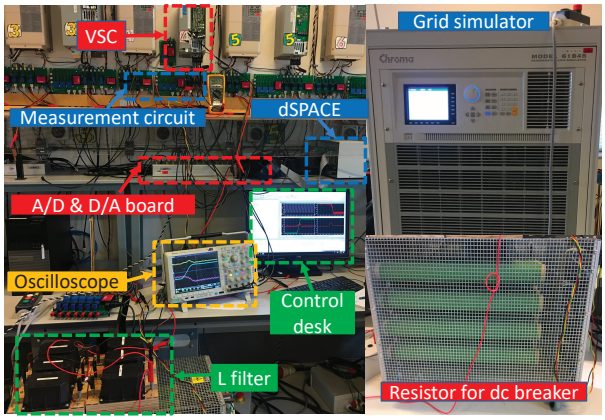

Fig. 13. Experimental setup at the Aalborg University.

the grid voltage is changed from 95 % to 105 % and $I_q^{'}$ is regulating 0.8 pu, and it can be observed that the experimental results have a similar tendency with the simulation ones. Fig. 16 shows the measured performance of the proposed method when there is 70 % of C parameter value in the control implementation. Compared with the result shown in Fig. 14(c), the performance with the proposed method is not affected by C variation in the control implementation since eq. (26), which relates to the physical system, does not change.Consequently, it is expected that all methods can operate in multi-pulse STATCOMs, and an enhanced performance can be achieved using the proposed PCH method.

V. Conclusions

We have introduced a tracking control law for a STATCOM system which is a special PCH form. The DEA method was used to regularize the system, which is a non-input-affine system to obtain the desired control input. The effectiveness of the proposed control strategy has been compared with the IOLMD and PI methods through simulations with power electronic devices and driving characteristics using Simscape Power Systems, MATLAB/Siumlink. From the simulation results, the proposed control strategy improved the transient performance of the system even in the inductive operating mode, where it has the lightly damped dynamics. Moreover, the proposed control strategy is robust against to the parameters uncertainties. Additional feedback damping will be designed to handle parameters uncertainty and/or disturbances in the future.

Acknowledgement

The authors would like to thank Prof. *Dong Eui Chang* of *Korea Advanced Institute of Science & Technology, Daejeon, South Korea* for the initial idea of the paper, Prof. *Wilsun Xu* of *University of Alberta, Edmonton, AB, Canada* for his insightful and constructive comments to improve the quality of the paper, and *Mr. Shih-Feng Chou* of *Aalborg University, Aalborg, Denmark* for the further experimental tests.

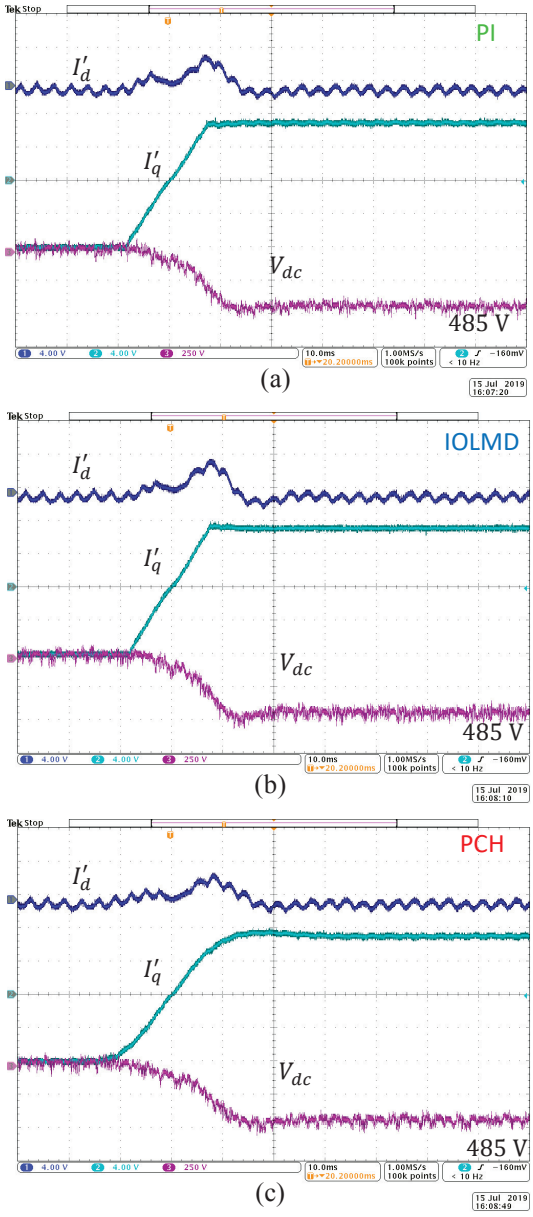

Fig. 14. Measured performance when $I_{q,ref}^{'}$ is changed from -0.8 pu to 0.8 pu., (a) PI, (b) IOLMD, (c) proposed method. Blue: $I_d^{'}$ [0.4 pu/div]; aqua: $I_q^{'}$ [0.4 pu/div]; bubble pink: V_{dc} [22.5 V/div].

References

[1] N. Hingorani, L. Gyugyi, and M. El-Hawary, *Understanding FACTS: Concepts and Technology of Flexible AC Transmission Systems*. IEEE press, New York, 2000.

[2] J. Rocabert, A. Luna, F. Blaabjerg, and P. Rodriguez, "Control of power converters in AC microgrids," *IEEE Trans. Power Electron.*, vol. 27, no. 11, pp. 4734–4749, 2012.

[3] Y. Gui, X. Wang, F. Blaabjerg, and D. Pan, "Control of grid-connected voltage-source-converters: Relationship between direct-power-control and vector-current-control," *IEEE Trans. Ind. Electron. Mag.*, vol. 13, no. 2, pp. 31–40, June 2019.

[4] T. K. Chau, S. S. Yu, T. Fernando, H. H. Iu, and M. Small, "A load-forecasting-based adaptive parameter optimization strategy of STATCOM using ANNs for enhancement of LFOD in power systems," *IEEE Trans. Ind. Informat.*, vol. 14, no. 6, pp. 2463–2472, June 2018.

[5] M. A. Soliman, H. Hasanien, H. Z. Azazi, E. E. El-kholy, and S. A. Mahmoud, "An adaptive fuzzy logic control strategy for performance

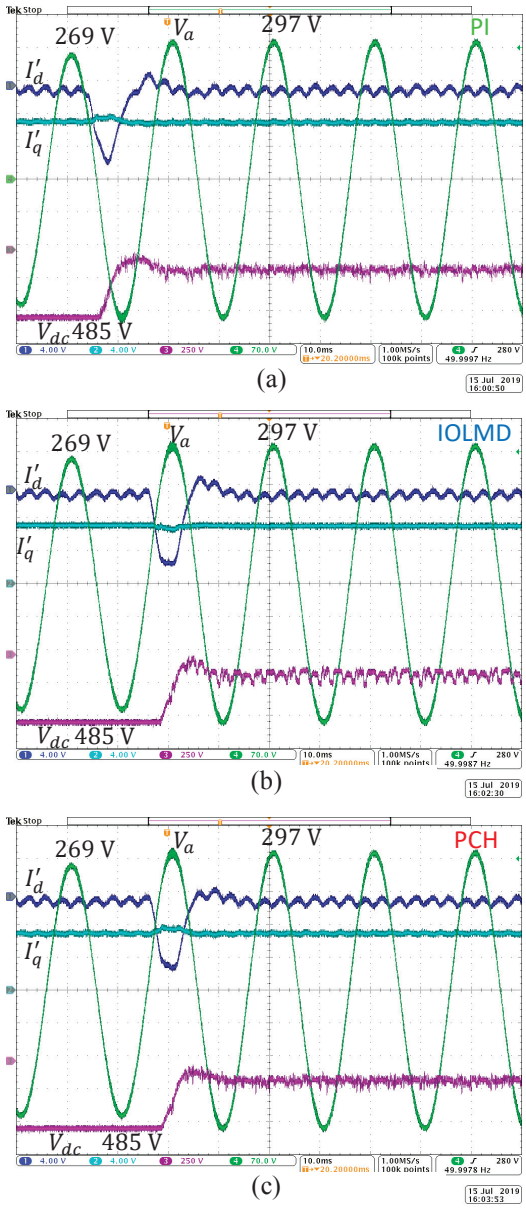

Fig. 15. Measured performance when the network voltage $V^{'}$ varies from 95% to 105%, (a) PI, (b) IOLMD, (c) proposed method. Blue: $I^{'}_d$ [0.4 pu/div]; aqua: $I^{'}_q$ [0.4 pu/div]; bubble pink: V_{dc} [22.5 V/div], green: V_a [70 V/div].

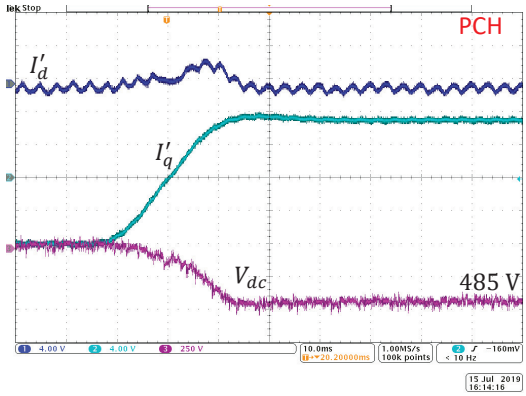

Fig. 16. Measured performance of the proposed method when there is 70 % of C parameter value in the control implementation. Blue: $I^{'}_d$ [0.4 pu/div]; aqua: $I^{'}_q$ [0.4 pu/div]; bubble pink: V_{dc} [22.5 V/div].

enhancement of a grid-connected PMSG-based wind turbine," *IEEE Trans. Ind. Informat.*, vol. 15, no. 6, pp. 3163–3173, June 2019.

[6] B. Singh, P. Jayaprakash, D. P. Kothari, A. Chandra, and K. Al Haddad, "Comprehensive study of DSTATCOM configurations," *IEEE Trans. Ind. Informat.*, vol. 10, no. 2, pp. 854–870, 2014.

[7] R. Xu, Y. Yu, R. Yang, G. Wang, D. Xu, B. Li, and S. Sui, "A novel control method for transformerless H-bridge cascaded STATCOM with star configuration," *IEEE Trans. Power Electron.*, vol. 30, no. 3, pp. 1189–1202, 2015.

[8] F. Shahnia, S. Rajakaruna, and A. Ghosh, *Static compensators (STATCOMs) in power systems*. Springer, 2015.

[9] B. Singh, R. Saha, A. Chandra, and K. Al-Haddad, "Static synchronous compensators (STATCOM): a review," *IET Power Electron.*, vol. 2, no. 4, pp. 297–324, 2009.

[10] Y. Xu and F. Li, "Adaptive PI control of STATCOM for voltage regulation," *IEEE Trans. Power Del.*, vol. 29, no. 3, pp. 1002–1011, 2014.

[11] C. Schauder and H. Mehta, "Vector analysis and control of advanced static VAR compensators," *IEE Proc. C (Gen. Transm. Distrib)*, vol. 140, no. 4, pp. 299–306, 1993.

[12] P. Petitclair, S. Bacha, and J.-P. Ferrieux, "Optimized linearization via feedback control law for a STATCOM," in *Proc. IEEE Ind. Appl. Soc. Annu. Meeting*, 1997, pp. 880–885.

[13] Y. O. Lee, Y. Gui, Y. Han, and C. C. Chung, "Stabilisation of asymmetrically structured back-to-back static synchronous compensator system with non-linear damping control," *IET Power Electron.*, vol. 8, no. 10, pp. 1952–1962, 2015.

[14] Y. Han, Y. O. Lee, and C. C. Chung, "Modified non-linear damping of internal dynamics via feedback linearisation for static synchronous compensator," *IET Gen. Transm. Distrib.*, vol. 5, no. 9, pp. 930–940, 2011.

[15] Y. O. Lee, Y. Han, and C. C. Chung, "Output tracking control with enhanced damping of internal dynamics and its output boundedness for STATCOM system," *IET Control Theory Appl.*, vol. 6, no. 10, pp. 1445–1455, 2012.

[16] Y. O. Lee and C. C. Chung, "Uniform output regulation via approximated input-output linearisation for lightly damped internal dynamics," *Int. J. Control*, vol. 86, no. 1, pp. 159–171, 2013.

[17] K. Wang and M. L. Crow, "Power system voltage regulation via STATCOM internal nonlinear control," *IEEE Trans. Power Syst.*, vol. 26, no. 3, pp. 1252–1262, 2011.

[18] A. Isidori, *Nonlinear Control Systems*, 3rd ed. New York: Springer Verlag, 1995.

[19] G. E. Valderrama, P. Mattavelli, and A. M. Stankovic, "Reactive power and imbalance compensation using STATCOM with dissipativity-based control," *IEEE Trans. Control Syst. Technol.*, vol. 9, no. 5, pp. 718–727, 2001.

[20] T.-S. Lee, "Lagrangian modeling and passivity-based control of three-phase AC/DC voltage-source converters," *IEEE Trans. Ind. Electron.*, vol. 51, no. 4, pp. 892–902, Aug 2004.

[21] H.-C. Tsai, C.-C. Chu, and S.-H. Lee, "Passivity-based nonlinear STATCOM controller design for improving transient stability of power systems," in *IEEE/PES Transm. Distrib. Conf. Exhib.*, 2005, pp. 1–5.

[22] Y. Gui, W. Kim, and C. C. Chung, "Passivity-based control with nonlinear damping for type 2 STATCOM systems," *IEEE Trans. Power Syst.*, vol. 31, no. 4, pp. 2824–2833, July 2016.

[23] Y. Chen, M. Wen, E. Lei, X. Yin, J. Lai, and Z. Wang, "Passivity-based control of cascaded multilevel converter based D-STATCOM integrated with distribution transformer," *Electr. Power Syst. Res.*, vol. 154, pp. 1–12, 2018.

[24] R. Ortega, A. van der Schaft, B. Maschke, and G. Escobar, "Interconnection and damping assignment passivity-based control of port-controlled Hamiltonian systems," *Automatica*, vol. 38, no. 4, pp. 585–596, 2002.

[25] H. Sira-Ramirez and Silva-Ortigoza, *Control design techniques in power electronics devices*. Springer-Verlag London Limited, 2006.

[26] J. Min, F. Ma, Q. Xu, Z. He, A. Luo, and A. Spina, "Analysis, design and implementation of passivity based control for multilevel railway power conditioner," *IEEE Trans. Ind. Informat.*, vol. 14, no. 2, pp. 415–425, 2018.

[27] X. Mu, J. Wang, W. Wu, and F. Blaabjerg, "A modified multifrequency passivity-based control for shunt active power filter with model-

parameter-adaptive capability," *IEEE Trans. Ind. Electron.*, vol. 65, no. 1, pp. 760–769, 2018.
[28] Z. Liu, Z. Geng, and X. Hu, "An approach to suppress low frequency oscillation in the traction network of high-speed railway using passivity-based control," *IEEE Trans. Power Syst.*, vol. 33, no. 4, pp. 3909–3918, 2018.
[29] Y. Gui, B. Wei, M. Li, J. M. Guerrero, and J. C. Vasquez, "Passivity-based coordinated control for islanded AC microgrid," *Appl. Energy*, vol. 229, pp. 551–561, 2018.
[30] S. Sastry, *Nonlinear Systems: Analysis, Stability, and Control*. Springer Verlag, 1999.

Yonghao Gui (S'11-M'17) received the B.S. degree in automation from Northeastern University, Shenyang, China, in 2009. He received the M.S. and Ph.D. degrees in electrical engineering from Hanyang University, Seoul, South Korea, in 2012 and 2017, respectively.

From February 2017 to November 2018, he worked with the Department of Energy Technology, Aalborg University, Aalborg, Denmark, as a Postdoctoral Researcher. Since December 2018, he has been working with the Automation & Control Section, Department of Electronic Systems, Aalborg University, Aalborg, Denmark, where he is currently an Assistant Professor. His research interests include control of Power Electronics in Power Systems.

Dr. Gui serves as an Associate Editor for the *IEEE Access* and the *International Journal of Control, Automation and Systems*. He was a recipient of the IEEE Power and Energy Society General Meeting Best Conference Paper Award in 2019.

C hung Choo Chung (S'91-M'93) received his B.S. and M.S. degrees in electrical engineering from Seoul National University, Seoul, South Korea, and his Ph.D. degree in electrical and computer engineering from the University of Southern California, Los Angeles, CA, USA, in 1993.

From 1994 to 1997, he was with the Samsung Advanced Institute of Technology, Korea. In 1997, he joined the Faculty of Hanyang University, Seoul, South Korea. He was an Associate Editor for the Asian Journal of Control from 2000 to 2002 and an Editor for the International Journal of Control, Automation and Systems from 2003 to 2005. He is currently An Associate Editor of journals including the IEEE Trans. on Control Systems Technologies, IEEE Trans. on Intelligent Transportation Systems, and IFAC Journal Mechatronics. Dr. Chung is currently a general co-chair of IEEE CDC 2020, to be held in Korea. He is also 2018 President-elect of Institute of Control, Robotics and Systems, Korea.

Frede Blaabjerg (S'86–M'88–SM'97–F'03) was with ABB-Scandia, Randers, Denmark, from 1987 to 1988. From 1988 to 1992, he got the PhD degree in Electrical Engineering at Aalborg University in 1995. He became an Assistant Professor in 1992, an Associate Professor in 1996, and a Full Professor of power electronics and drives in 1998. From 2017 he became a Villum Investigator. He is honoris causa at University Politehnica Timisoara (UPT), Romania and Tallinn Technical University (TTU) in Estonia.

His current research interests include power electronics and its applications such as in wind turbines, PV systems, reliability, harmonics and adjustable speed drives. He has published more than 600 journal papers in the fields of power electronics and its applications. He is the co-author of four monographs and editor of ten books in power electronics and its applications.

He has received 32 IEEE Prize Paper Awards, the IEEE PELS Distinguished Service Award in 2009, the EPE-PEMC Council Award in 2010, the IEEE William E. Newell Power Electronics Award 2014, the Villum Kann Rasmussen Research Award 2014 and the Global Energy Prize in 2019. He was the Editor-in-Chief of the IEEE TRANSACTIONS ON POWER ELECTRONICS from 2006 to 2012. He has been Distinguished Lecturer for the IEEE Power Electronics Society from 2005 to 2007 and for the IEEE Industry Applications Society from 2010 to 2011 as well as 2017 to 2018. In 2019-2020 he serves a President of IEEE Power Electronics Society. He is Vice-President of the Danish Academy of Technical Sciences too. He is nominated in 2014-2018 by Thomson Reuters to be between the most 250 cited researchers in Engineering in the world.

Mads Graungaard Taul (S'17) received the B.Sc. and M.Sc. degree in Energy Technology with specializing in Electrical Energy Engineering and Power Electronics and Drives from Aalborg University, Denmark in 2016 and 2019, respectively. In connection with his M.Sc. degree in 2019, he received the 1st prize master's thesis award for excellent and innovative project work by the Energy Sponsor Programme. Currently, he is pursuing a Ph.D. in Power Electronic Systems with the Department of Energy Technology at Aalborg University, Denmark. His main research interests include renewable energy sources and grid-connected converters with a special focus on modeling and control of power electronics-based power systems under grid fault conditions.